Ghosh Gargi (Orcid ID: 0000-0003-1328-2425)

Engineering tumor constructs to study matrix-dependent angiogenic signaling of breast cancer cells

Malak Nasser, Gargi Ghosh*

Bioengineering Program, Department of Mechanical Engineering

University of Michigan-Dearborn

*Corresponding Author: email address: gargi@umich.edu

Phone: 313-593-5013

Fax: 313-593-3851

This is the author manuscript accepted for publication and has undergone full peer review but has not been through the copyediting, typesetting, pagination and proofreading process, which may lead to differences between this version and the Version of Record. Please cite this article as doi: 10.1002/btpr.3250

Abstract

Breast cancer is the leading cause of cancer deaths among females globally. The crosstalk between tumor microenvironment and neoplastic cells is the key for promoting tumor growth, stimulating tumor angiogenesis, and metastasis to distant organs. Thus, it is highly important to investigate tumor cell-matrix interactions to facilitate screening of different anti-cancer agents, individually or in combination. We, herein report, the development of an *in vitro* three-dimensional (3D) breast cancer model to investigate the effect of stromal crosslinking and consequent, stiffening on the angiogenic activity of cancer cells. Crosslinking of collagen gels was altered via non-enzymatic glycation and highly aggressive breast cancer cells, MDA-MB-231, were encapsulated in these gels. Cells encapsulated in glycated/stiffer matrices displayed an increased expression of pro-angiogenesis-related signals. Inhibition of mechanotransduction pathways on the angiogenic activity of aggressive tumor cells in stiff matrices was investigated using Y-27632, blebbistatin, and cytochalasin D. Rho-associated kinase (ROCK) inhibitor, Y-27632, diminished the pro-angiogenic signaling, thereby suggesting the potential dependence of breast cancer cells on the Rho/ROCK pathway in regulating tumor angiogenesis. Our findings highlight the potential of the developed model to be used as a tool to investigate matrix-associated tumor angiogenesis and screen different therapeutic agents towards inhibiting it.

Keywords: Breast cancer; Angiogenesis; Mechanotransduction; Microenvironment; Hydrogel

Introduction

Breast cancer is the most frequently diagnosed cancer and the leading cause of cancer death among females worldwide (1). When diagnosed early or at a localized stage, the five-year survival rate increases to 98% as compared to a 27% survival rate after metastases (2). When tumors begin to grow beyond 1-2 mm^3, the diffusion of nutrients and oxygen into the native tissue becomes insufficient to support the insatiable metabolic demands required for the continued growth and survival of the tumor cells (3). Consequently, the cells release a combination of angiogenic factors to recruit endothelial cells from neighboring blood vessels and induce the formation of new blood capillaries, not only to provide the cells with the necessary oxygen and nourishment required for the cells' continued growth, but also to provide an avenue through which these cells can migrate and reach distant organs in the body (4). Therefore, angiogenesis, i.e. the formation of blood vessels from pre-existing vessels, becomes the rate-limiting step for tumors to grow and metastasize (5). Specifically, a change in the balance between regulatory pro- and anti- angiogenic factors, leading to the increase in the net stimulatory activity and the onset of angiogenesis, triggers metastatic tumor growth (6).

Recent inquiries into tumor progression allude to the importance of microenvironmental cues in stimulating the aggressive phenotype of cancer cells (7, 8). As a major component of tumor microenvironment, extracellular matrix (ECM) is believed to play an important role in tumor development and metastasis (7, 8). The ECM is a complex network consisting of distinct macromolecules which result in a matrix with specific physical, biochemical, and mechanical properties (9). Together, these properties provide the structural support for the cellular components of tissues and pertain to the signaling mechanisms that determine the cell's ability to sense and react to external mechanical forces, thereby actively regulating cell behavior and contributing to

tumor progression (9-12). Type I and IV collagen proteins are the most prevalent components of the ECM providing the main structural support for the interstitial matrix and the key component of the basement membrane, respectively (13, 14). Typically, tumor tissue undergoes continuous remodeling of the ECM, due to elevated production, deposition, and altered organization of collagen and related macromolecules, in tandem with increased metalloproteinase (MMP) activity (12). Cancer cells recognize the change in ECM crosslinking/increase in matrix stiffness and respond by generating increased traction forces on their surroundings through actomyosin and cytoskeleton contractility (15). This leads to a series of signaling cascades that regulate gene expression and result in enhanced cancer cell growth and migration and contribute to the invasive phenotype, commonly associated with tumors (16).

Despite the importance of stroma remodeling/stiffening in tumor progression, how the microenvironmental cues are co-opted in the angiogenic response of the cancer cells remains unclear. In our previous studies, using mechanically tuned hydrogels we demonstrated that the matrix stiffening not only promotes cell proliferation and migration of the highly aggressive breast cancer cell line, MDA-MB-231, but it also correlates with higher levels of vascular endothelial growth factor (VEGF) expression (17). Another recent study has reported upregulated VEGF expression by hepatocellular carcinoma (HCC) cells when cultured on stiffer matrices (18). Together, these studies suggest the potential existence of a regulatory mechanotransduction pathway that may govern the angiogenic activity of tumor cells. We hypothesize that ECM remodeling leading to stiffening during tumor progression regulates the pro-angiogenic signaling of cancer cells and interruptions in the mechanotransductive pathway may have a therapeutic potential in disrupting vascularization and slowing tumor progression.

In our study, collagen-based matrices were prepared to develop 3D breast cancer model for studying matrix-dependent angiogenic activity of cancer cells. We used a non-enzymatic glycation approach to increase crosslinking and consequently, the stiffness of the gels while keeping the collagen density constant. Aggressive breast cancer cells, MDA-MB-231, were encapsulated within these gels and the release of angiogenic factors was profiled. Further, to validate the developed model, the efficacy of inhibitors, targeting different mechanotransduction pathways, in impairing the angiogenic signaling of cancer cells was studied.

Materials and Methods

2.1 Materials

Rat tail high concentration collagen type I was obtained from Corning (Bedford, MA). Sodium hydroxide, fluorescein isothiocyanate-dextran of 150K MW (FITC-dextran), sodium acetate, cysteine hydrochloride, sodium phosphate monobasic, sodium phosphate dibasic, papain suspension, cytochalasin D, and (-)-blebbistatin were procured from Sigma Aldrich (St. Louis, MO). Y-27632 and Na_2EDTA were purchased from EMD Millipore (Kankakee, IL). Dulbecco's Phosphate Buffer Saline (DPBS), RPMI Medium 1640, Penicillin-Streptomycin (Pen Strep), 0.25% Trypsin-EDTA, fetal bovine serum (FBS), and collagenase Type I were acquired from Gibco by Life Technologies (Grand Island, NY). D-(-)-Ribose, Hoechst 33342, and Alexa Fluor™ 488 phalloidin were obtained from Thermofisher Scientific (Waltham, MA). AlamarBlue™ cell viability reagent was purchased from Invitrogen by Thermo Fisher Scientific (Eugene, OR). Acetone, methanol, and glacial acetic acid were acquired from Fisher Chemical (New Jersey). Endothelial cell basal medium-2 (EBM-2) and EGM-2 SingleQuots growth factors were obtained from Lonza (Walkersville, MD).

2.2 Fabrication of Collagen gels

To fabricate mechanically tunable gels without altering the protein concentration, non-enzymatic pre-glycation of collagen, known as Maillard reaction, was carried out as described earlier (19). Briefly, collagen stock solutions were mixed with 500 mM ribose to form glycated collagen solutions with a final concentration of 0, 50, 100, 200, and 250 mM ribose in 0.02N acetic acid and incubated for 5 days at 4℃ (19). Following pre-glycation, collagen gels were fabricated according to the manufacturer's protocol. Briefly, glycated collagen solutions were neutralized with 1M sodium hydroxide (NaOH) in 10X DPBS and diluted with distilled water. Collagen gels were formed by adding 250 µL of the neutralized solution to the wells of a 48-well plate and allowed to cross-link for 30 minutes in an incubator at 37℃ to form gels with a final collagen concentration of 1.5 mg/mL.

2.3 Characterizations of Collagen gels

2.3.1 Degradation

To measure the rate of collagen gel degradation, the samples were incubated in 2.5 units/mL collagenase type I solution on a rotator shaker at room temperature. The weights of the gels were measured each day for 10 days, consecutively. The degradation ratio was calculated by normalizing the weights of the samples at each day to the weights of the samples on the day of fabrication.

2.3.2 Swelling Ratio

To measure the swelling ratio (Q_m) of the collagen gels, the samples were incubated in DPBS for 72 h on a rotator shaker at room temperature following gel formation. The weights of the hydrated gels were measured (W_{wet}). The hydrogels were then dried at 37℃ overnight, and their weights

(W_{dry}) were measured. The swelling ratio of the hydrogels was then calculated using the following equation:

$$Q_m = \frac{W_{wet}}{W_{dry}}$$

2.3.3 Diffusion

To measure the rate of diffusion of macromolecules from the gels, FITC-dextran molecules of 150KDa MW were added to the neutralized collagen gel solution at a concentration of 50 µg/mL (w/v), and the collagen gels were fabricated after incubation for 30 min at 37℃. The gels were washed and incubated in DPBS for seven days. Each day, the buffer solution containing the diffused molecules was collected and replaced with 500 µL of fresh DPBS. The fluorescence intensity for each sample was measured using SpectraMax M3 Multi-Mode Microplate Reader at excitation/emission wavelengths 495/519 nm. The diffusive release was calculated as a percentage using the following equation:

$$Release\ (\%) = 100 \times \frac{Amount\ of\ dextran\ molecules\ released\ each\ day\ (g)}{Amount\ of\ dextran\ molecules\ in\ the\ gel\ after\ wash\ (g)}$$

The release data of dextran was mathematically fitted to the following kinetic models: zero-order, first-order, and Higuchi model. The best fit was evaluated from the correlation co-efficient. Additionally, to determine the mechanism of macromolecule release through the collagen gels, the release data was fitted to Korsmeyer-Peppas model:

$$F = \frac{M_t}{M_0} = kt^n$$

where F is the fractional release of the molecule, M_t is the amount of dextran diffused at any time, M_0 is the total initial amount of dextran that was encapsulated within the gels, k is the kinetic constant, t is time, and n is the diffusional exponent. Where $n \leq 0.5$, the transport of macromolecules can be defined by Fick's diffusion alone. Where $0.5 > n \leq 0.9$, the transport of

molecules is governed by both diffusion and polymer relaxation/erosion, and for $n > 0.9$, polymer relaxation/erosion define the release of molecules. The data fitting was carried out for $\frac{M_t}{M_0} = 60\%$. At least three independent experiments were performed with five replicates per experiment.

2.3.4 Scanning Electron Microscope

Collagen gels were dried overnight at 50°C. The dried samples were subjected to gold sputtering for 7 seconds. Images of the collagen fibers and pores were then captured using Zeiss scanning electron microscope (LEO 1455 VP).

2.4 Cell Culture and Angiogenic Activity

Highly invasive breast cancer cells (MDA-MB-231) were purchased from American Type Culture Collection (ATCC) and expanded in RPMI 1640 Medium supplemented with 10% (v/v) fetal bovine serum (FBS) and 1% (v/v) penicillin-streptomycin. Human umbilical vein endothelial cells (HUVECs) were obtained from (ATCC) and expanded in endothelial cell nasal medium-2 (EBM-2) supplemented with 1% (v/v) penicillin-streptomycin and EGM-2 SingleQuot (containing FBS, hydrocortisone, hFGF, VEGF, R3-IGF-1, ascorbic acid, hEGF, GA-100, and heparin). Cells were cultured and incubated at 37°C and 5% CO_2. In this study, MDA-MB-231 and MCF-7 cells were used up to passage 7. HUVECs were used up to passage 6.

2.4.1 Cell Proliferation

Following detachment from the flasks using 0.25% Trypsin-EDTA, resuspended cancer cells were incorporated into the collagen gels by adding the cells to neutralized collagen solutions at a density of 12.5 x 10^4 cells/gel and incubated in 300 µL of serum-free media at 37 °C and 5% CO_2 after gel formation. Collagen gels were collected and frozen immediately after gels were formed, and again after 2, 4, and 6 days. The collected samples were digested with papain solution at 37 °C for 3 h. The papain solution was created by dissolving 0.1M sodium acetate, 0.01M Na_2EDTA, and

0.005M cysteine hydrochloride in 0.2M sodium phosphate buffer (consisting of sodium phosphate monobasic and sodium phosphate dibasic) and adding papain suspension. Cell proliferation was assessed using Quant-iT™ dsDNA High-Sensitivity Assay Kit (Thermo Fisher, USA). The fluorescence intensity was then measured using SpectraMax M3 Multi-Mode Microplate Reader at excitation/emission wavelengths 480/530 nm. Cell proliferation over time was calculated as a percentage by dividing the fluorescence intensity of the gels at each day over the day of fabrication using the following equation:

$$Normalized\ Cell\ Growth\ (\%) = 100 \times \frac{RFU_{Any\ Day}}{RFU_{Day\ 0}}$$

The data was collected from at least three-independent experiments, each of which was carried out in three replicates.

2.4.2 Immunostaining

Cancer cells incorporated into collagen gels at a cell density of 2.5 x 10^4 cells/gel were stained with 1% (v/v) Hoechst 33342 dye for 5 min. The cells were then fixed and permeabilized with 1:1 acetone:methanol solution at -20℃ for 20 min. The cells were then blocked with 5% (w/v) BSA solution for 1 h, washed with 1X DPBS three times, and incubated with 2.5% (v/v) Alexa Fluor 488-phalloidin antibody for 1 h at 37℃. Following which, the cells were washed three times with 1X DPBS, and images were captured using Olympus laser scanning confocal microscope (FV 1200) to visualize the actin arrangement of the cell.

2.4.3 Quantification of released angiogenic-related factors

To quantify the release of angiogenic factors by cancer cells as a function of microenvironment, cells were encapsulated within collagen gels at a density of 12.5 x 10^4 cells/gel in 48 well plates and incubated in serum-free media. Four days post-fabrication, the spent media was collected and concentrated using Vivaspin 2 (2000 MWCO) centrifugal concentrators. Angiogenic molecules in

the media were measured via Proteome Profiler™ Human Angiogenesis Array from R&D Systems. Bio-Rad Molecular Imager with ChemiDoc XRS+ Imaging System was used to image the membranes and the average intensity of each angiogenic factor was measured using the Image Lab Software (Version 4.1). The angiogenesis array was run two times.

2.4.4 Proliferation of HUVECs

HUVECs were seeded in 96 well plates at a density of 1 x 10^4 cells/well and incubated in the presence of concentrated media (collected from encapsulated cancer cells after 4 days) containing released angiogenic factors at 37°C and 5% CO_2. Cells incubated in endothelial cell growth media and serum-free RPMI media served as the positive and negative controls, respectively. After 48 h of incubation, AlamarBlue cell viability reagent was added to fresh media and allowed to incubate for 3.5 h at 37°C and 5% CO_2, and the fluorescence intensity was then measured using SpectraMax M3 Multi-Mode Microplate Reader at excitation/emission wavelengths 570/595 nm. Cell growth was then calculated as a percentage using the equation below:

$$Normalized\ Cell\ Growth\ (\%) = 100\ x\ \frac{(RFU_{sample} - RFU_{blank})}{RFU_{control}}$$

The data was collected from at least three independent experiments with three replicates per experiment.

2.5 Inhibition of Mechanotransduction Pathways

Cancer cells were encapsulated within glycated (stiff) collagen gels at a density of 12.5 x 10^4 cells/gel and incubated in serum-free media for 48 h at 37°C and 5% CO_2. Following which, serum-free media containing either 10μM of Y-27632, 50 μM of Blebbistatin, or 1μM of Cytochalasin D, inhibitors targeting different mechanotransduction pathways, were added to the cells for 48 h. Cells incubated in serum-free media without any inhibitors served as the control. The viability of

the cells was assessed using AlamarBlue™ Cell Viability Reagent to ensure that the inhibitors were not toxic to the cells. Following incubation for 48 h, the media was collected, concentrated, and the profile of the released angiogenic factors was assessed via Proteome Profiler™ Human Angiogenesis Array from R&D Systems.

2.6 Statistical Analysis

All experiments were conducted at least in triplicates and repeated three times. The data represents the mean ± S.E.M of three independent experiments. Statistical analyses were carried out using one way ANOVA with post-hoc Tukey HSD test. Differences between two sets of data were considered significant at p-value < 0.05.

Results

Non-enzymatic glycation is carried out through the Maillard reaction, where the aldehyde group on reducing sugars reacts with amino groups on collagen. The reaction produces a Schiff base which forms Amadori products that eventually form glycation end products. The accumulation of these end products in tissues results in a change in their mechanical and biochemical properties, as observed in conditions such as aging and diabetes (19).

3.1 Fabrication and Characterization of Collagen Hydrogels

The crosslinking of the collagen hydrogels was altered via non-enzymatic pre-glycation of 1.5 mg/mL collagen with 250 mM ribose. The alteration of crosslinking via increase in ribose concentration had been demonstrated to increase the compressive modulus of the hydrogels from approximately 175 Pa (non-glycated) to 730 Pa (glycated with 250 mM ribose) (20). In this study, the integrity of the collagen gels was assessed by measuring enzymatic degradation profiles in the presence of collagenase. Over the 10-day period, a decrease in the normalized weights of the gels was observed, irrespective of ribose treatment (Fig 1A). This decrease in weights corresponded to

their degradation in presence of collagenase. However, all the gels retained their physical integrity over the course of the 10 days indicating that the pre-glycation has no effect on the integrity of the gels (p-value > 0.05).

The effect of pre-glycation treatment on the swelling ratio of the collagen gels was also investigated. The swelling ratio of the gels decreased from 73.8 ± 10.9 (collagen gels without ribose treatment) to 49.6 ± 6.5 (collagen treated with 250 mM ribose), although the change was not significant different (p-value > 0.05). In addition, the internal microstructure of the collagen gels was also studied using scanning electron microscopy. The ribose treatment resulted in more prominent and larger/thicker collagen fibers (Fig 1B) possibly due to aggregation resulting from Maillard reaction. Our observations are in agreement with earlier studies (20). Considering that collagen concentration and consequently, cell-adhesive sites are same for non-glycated as well as the glycated gels, thicker fibers suggest enhanced local cell adhesion sites (21). To assess whether non-enzymatic pre-glycation altered the free volume available for transport of macromolecules across the hydrogels, the macromolecular release kinetics was investigated. For the purpose, collagen disks (with or without incubation with 250 mM ribose) were fabricated encapsulating FITC-conjugated (150kDa) dextran. Figure 1C demonstrates no significant difference in the cumulative release (% release) of dextran over a span of 7 days as a function of ribose treatment. The release data were fitted to various kinetic models. Higuchi and Korsemeyer-Peppas models/equations fitted better, as manifested from the correlation coefficients (Table 1), irrespective of collagen glycation. Further, the average values of diffusional exponent (n) for the collagen gels, obtained from Korsemeyer-Peppas model, were found to be greater than 0.5, but less than 0.9 (Table 1), thereby suggesting that the transport of macromolecules across the gels is via, non-Fickian or anomalous transport. This refers to a combination of both, diffusion as well as

polymer relaxation/erosion. No significant difference (p-value > 0.05) in dextran release profile from either of the collagen hydrogels indicates that ribose treatment did not affect the transport of macromolecules. Taken together, these studies highlight that pre-glycation altered the crosslinking and mechanical properties of the gels without impacting the integrity or swelling ratio of collagen matrices. This further suggests that any difference observed in cellular behavior/secretory activities will be primarily due to altered cell-matrix interactions resulting from altered ECM crosslinking.

3.2 Effect of Matrix Stiffness on Cancer Cell Behavior

To study the impact of ECM crosslinking and subsequent stiffening on cellular behavior, highly invasive breast cancer cells (MDA-MB-231) were encapsulated within collagen gels of varying pre-glycation. DNA quantification was used to assess the cell proliferation 2-, 4-, and 6-days post encapsulation. As observed in Fig 2A, cells remained viable and an increase in cell growth was observed irrespective of gel glycation compared to day 0 (p-value < 0.05). Moreover, no difference in cell growth was observed between glycated and non-glycated gels (p-value> 0.05) indicating collagen glycation does not impact the proliferative potential of the cancer cells.

To assess whether modulating collagen crosslinking/gel stiffness caused any morphological changes of cancer cells, four days post-fabrication, the F-actin cytoskeleton of MDA-MB-231 cells was stained by Alexa Fluor 488 conjugated phalloidin antibody. The confocal images (Fig 2B) demonstrated primarily round cells with very few cells with invadopodia in the non-glycated gels. On the other hand, in case of glycated gels, the cells with invadopodia were the majority with very few displaying a round or blebbing phenotype.

3.3 Effect of Matrix Stiffness on Angiogenesis

To investigate how collagen glycation/gel stiffness influences the release of angiogenic factors by the cancer cells, four days post-fabrication, the conditioned media was collected and the angiogenic molecules were measured via Proteome Profiler Human Angiogenesis. The release of pro-angiogenic molecules by MDA-MB-231 cells encapsulated within collagen gels treated with 250 mM ribose was compared with those encapsulated with collagen gels without treatment with ribose (0 mM) (Fig 3A). As observed, glycated (stiffer) gels stimulated angiogenic signaling of the cancer cells as manifested from enhanced secretion of pro-angiogenesis related factors. In addition, multiple pro-angiogenesis factors including angiogenin, angiopoietin-1, CXCL16, EGF, EG-VEGF, endoglin, FGF acidic, FGF basic, FGF-4, FGF-7, HGF, Leptin, MCP-1, MMP-8, PDGF-AA, PDGF-AB/PDGF-BB, PIGF, VEGF-C were released only when the cells were encapsulated within glycated/stiffer gels. On the other hand, comparison of secretion of anti-angiogenic molecules revealed no drastic difference in the secretory signatures of cancer cells when matrix crosslinking/stiffness was altered (Fig 3B). Few anti-angiogenesis factors including ADAMTS-1, angiostatin/plasminogen, endostatin/collagen XVIII, platelet factor 4, serpin B5, and vasoinhibin were released only by cells encapsulated within the stiffer gels, albeit the expression level was very low. Further, for quantitative analysis of angiogenic signaling of MDA-MB-231 cells, the signal intensities of the pro-angiogenic factors released by the cells encapsulated within glycated gels were normalized with respect to the non-glycated gels. The expression levels of multiple pro-angiogenic molecules including activin A, amphiregulin, artemin, IL-1β, persephin, uPA, and VEGF were upregulated (normalized values > 1.5) (Fig 3C) whereas the expression levels of anti-angiogenic molecules remained unchanged (0.5 < normalized values < 1.5) (Fig 3D).

To study the effect of this angiogenic cocktail on the proliferation of endothelial cells, conditioned media was collected 4 days post-encapsulation of MDA-MB-231 cells within collagen

gels. HUVECs were seeded at a density of 1 x 10^4 cells/well in 96 well plates in the presence of conditioned media, and their cell growth was assessed using Alamar Blue Cell Viability Reagent. HUVECs cultured in presence of supplemented endothelial cell growth media and serum-free RPMI media acted as the positive and negative controls, respectively. To quantitatively assess the effect of conditioned media on growth of HUVECs, proliferation of cells was normalized with respect to cells incubated in supplemented endothelial cell media. Figure 3E shows an increase in growth of endothelial cells in the presence of conditioned media collected from MDA-MB-231 cells incubated in the stiffer gel.

3.6 Effect of Mechanotransduction Inhibitors on Angiogenesis

The impact of inhibition of mechanotransduction pathways on angiogenic activity of cancer cells was explored. Towards this goal, 10 μM Y-27632, 50 μM blebbistatin, and 1 μM cytochalasin D were added to aggressive breast cancer cells embedded within stiff collagen matrices. Y-27632 is a widely used Rho/ROCK inhibitor that binds to the catalytic site of these kinases thereby inhibiting their activity and the formation of stress fibers (22). Blebbistatin is a myosin II inhibitor that binds to the myosin-ADP-P_i complex and interferes with the phosphate release process, thereby preventing proper crosslinking of actomyosin (23). Cytochalasin D is a widely used actin inhibitor that inhibits both the polymerization and depolymerization of actin subunits by binding to actin filament ends (24). After 48 h of incubation with the inhibitors, the serum-free media was collected and assessed for the released angiogenic factors. Figure 4A shows the normalized signal intensities of the factors released by cells from gels in presence of inhibitors with respect to those released in the absence of inhibitors. Y-27632, downregulated the expression of multiple molecules including angiogenin, angiopoietin-1, amphiregulin, artemin, FGF acidic, GDNF, GM-CSF, IGFBP-1, IL-1β, MIP-1a, MMP-8, PD-ECGF, PDGF-AA, PDGF-AB/BB, uPA, VEGF (pro-

angiogenic factors) (Fig 4A). On the other hand, in the presence of blebbistatin and cytochalasin D, the expression of the angiogenic factors primarily remained unchanged; however, secretion of few factors including IL-8, MIP-1a, and PD-ECGF was upregulated. The cell viability was tested to assess whether the alteration in angiogenic signaling is due to the cytotoxicity of the pharmacological inhibitors. However, no difference in the viability of the cells incubated in the presence of different inhibitors was observed when compared to those incubated in the absence of inhibitors (Fig 4B). This suggests that differential expression of angiogenesis-related factors by MDA-MB-231 in the presence of pharmacological inhibitors can be attributed only to the inhibition of mechanotransduction events.

Discussion

Recent studies attempting to better understand the factors influencing tumor progression have drawn attention to components of the tumor microenvironment, specifically the ECM. The continuous remodeling of the ECM contributes to a stiffer matrix in tumor tissue, thereby activating signaling pathways that stimulate tumor progression through increased cell proliferation and migration (16). However, little is known about how this increased stiffness affects the signaling pathways that control the angiogenic activity of cancer cells. Breast tissue, considered a soft tissue under physiological conditions, stiffens markedly with tumor development leading to alteration in the micro-environmental physical forces (25, 26). In this current study, we sought to understand how this matrix stiffening alters the pro-angiogenic activity of cancer cells and whether inhibition of mechanotransduction permit regulating their stiffness-dependent secretory activity. Towards this goal, we developed 3D scaffolds of varying compliances (175 kPa and 730 kPa) using a non-enzymatic pre-glycation approach. The highly aggressive breast cancer cells (MDA-MB-231) were encapsulated in the collagen gels and the angiogenesis-related factors secreted by

the cells were profiled. The increase in stiffness translated to the expression of multiple pro-angiogenic factors that were not expressed by the cells encapsulated in the compliant gels (angiogenin, angiopoietin-1, FGF acidic, basic, FGF-4, and FGF-7, PDGF, CXCL16, EGF, EG-VEGF, Endoglin, HGF, Leptin, MCP-1, MMP-8, PDGF-AA, PIGF, VEGF-C) along with an upregulation of several pro-angiogenic factors that were expressed in both including activin A, amphiregulin, artemin, IL-1β, persephin, uPA, and VEGF. Our observations are consistent with other studies (17, 27-29) that demonstrated matrix-stiffness dependent alteration of angiogenic signaling of different cell lines. Our earlier studies have demonstrated that human bone marrow derived MSCs prefer matrices of optimal stiffness for maximal expression of VEGF (27). On the other hand, human dermal fibroblasts exhibited a preference for compliant matrices for optimal angiogenic activity (28). Similarly, the matrix-stiffening mediated enhanced secretion of angiogenic factors by lung cancer cells as well as breast cancer cells (17, 29).

In tumors, VEGF is secreted by cancer cells and surrounding stroma and contributes to tumor progression and invasion, increased blood vessel density, and metastasis (30, 31). Moreover, VEGF and PDGF both play a role in inducing intussusceptive angiogenesis, a process found in many cancers including breast cancer (30). The upregulation of MMP (matrix metalloproteinase) and uPA (urokinase plasminogen activator) in the stiffer matrices is of key significance as they have been shown to modulate VEGF-mediated cell invasion by degrading the basal membrane and extracellular matrix and allowing endothelial cells to migrate and form sprouts (30, 32). FGF has been shown to not only play a role in tumor angiogenesis, but also have a role in initiation or promotion of tumorigenesis (33). Angiogenin, which was only expressed by cells in the stiffer matrix promotes tumoral growth and angiogenesis (34), and angiopoietin-1 stimulates vessel maturation and their stabilization (30). Leptin, the hunger-inhibiting hormone, was also expressed

only by the cells encapsulated in the stiffer matrix, and studies have highlighted its role in breast carcinogenesis as it affects ER signaling and aromatase activity (35-37). In our study, amphiregulin, which is an EGF-related peptide, was overexpressed by highly aggressive MDA-MB-231 cancer cells encapsulated in stiffer matrices. This is consistent with other studies where the frequency and levels of amphiregulin expression are generally higher in invasive breast tumors than in localized carcinoma or in normal breast tissue (38).

Earlier studies have shown that the altered mechanical cues from the microenvironment enhance integrin clustering and recruitment of focal adhesion proteins and subsequently alter cytoskeletal organization (12, 39). In this study, we observed formation of actin-based protrusion of plasma membranes when MDA-MB-231 cells were encapsulated within the glycated/stiffer gels, thereby suggesting that the differential secretory responses of MDA-MB-231 cells may be partly related to the cell contractility or cytoskeletal reorganization. The local interactions between F-actin, myosin filaments, and various crosslinking proteins govern force generation, dynamics, and reorganization of the intracellular cytoskeleton. The cytoskeleton is responsible for many essential cellular functions including migration, adhesion, and mechanotransduction (40). We utilized different mechanotransduction inhibitors to evaluate their effect on angiogenic signaling of cancer cells. Our study demonstrated that ROCK inhibitor, Y-27632, downregulated the expression of the pro-angiogenic factors, suggesting the involvement of ROCK signaling pathway in the stiffness-dependent pro-angiogenic signaling of MDA-MB-231 cells. On the contrary, blebbistatin and cytochalasin D did not influence the expression of most of the pro-angiogenic molecules and upregulated the expression of few. Although this was somewhat unexpected, we anticipate that different mechanisms by which actin filament disruptors and the Rho kinase inhibitor affect the cytoskeleton may play a role in the angiogenic activity of the cancer cells. Y-

27632 is a specific inhibitor of ROCK activity. As a major effector of RhoA, ROCK modulates actin cytoskeleton organization, stress fiber formation, and smooth muscle contraction via phosphorylation of myosin light chain (MLC) and LIM kinase (LIMK) and has been associated with matrix-stiffness induced mechanotransduction (22). Blebbistatin selectively inhibits non-muscle myosin II in an actin-detached state (23) thereby inhibiting ATP-binding required for motor activity and actin cross-linking, independently of MLC phosphorylation (41). On the other hand, cytochalasin D inhibits actin polymerization and induces depolymerization of actin filaments (24). Our data show that neither the inhibition of non-muscle myosin II nor the inhibition of actin polymerization govern the pro-angiogenic signaling of MDA-MB-231 cells. Instead, we show that the angiogenic activity of the breast cancer cells is dependent on the activation of Rho/ROCK pathway. Our study implies that stromal crosslinking influences the paracrine signaling of cancer cells and inhibiting the ability of the cells to sense the alteration of matrix stiffness may decrease their angiogenic activity. The model, thus developed, can be a powerful tool in identifying agents capable of interrupting the mechanotransduction pathways that can potentially regulate tumor angiogenesis. Further modifications via inclusion of endothelial cells as well as pericytes to obtain a more physiologically relevant model may permit screening of anti-angiogenic agents, individually or in combination of mechanotransduction inhibitors.

Conclusion

Identification of new signaling hubs regulating angiogenic signaling of cancer cells will permit development of novel therapeutic interventions. In this study, the tumor model with varying matrix crosslinking/stiffness was developed to investigate the influence of matrix stiffness in guiding pro-angiogenic signaling of breast cancer cells and the potential of the model to screen the inhibitors of mechanotransduction pathways that can regulate angiogenic activity of cancer cells. Our study

demonstrated matrix-dependent upregulation of angiogenic activity of breast cancer cells and that inhibition of mechanotransduction pathway, especially via interruption of Rho/ROCK pathway via Y-27632 abated their angiogenic potential. The study highlights that the tumor model can be used for studying the effect of microenvironment on cancer cell behavior/characteristics and for screening newly developed or existing anti-angiogenic agents, individually or in presence of interrupters of mechanotransduction pathways.

Funding Sources

The authors would like to thank NIH (1R03EB026526-01) and Alternatives Research and Development Foundation (AWD005747 and AWD007781) for the financial support.

Declaration of Interest

The authors declare that they do not have any conflict of interest to disclose.

References

1. Sung H, Ferlay J, Siegel RL, Laversanne M, Soerjomataram I, Jemal A, Bray F. Global Cancer Statistics 2020: GLOBOCAN Estimates of Incidence and Mortality Worldwide for 36 Cancers in 185 Countries. *CA Cancer J Clin*. 2021; 71: 209-249. doi: 10.3322/caac.21660.
2. Howlader N, Noone AM, Krapcho M, Miller D, Brest A, Yu M, Ruhl J, Tatalovich Z, Mariotto A, Lewis DR, Chen HS, Feuer EJ, Cronin KA. SEER Cancer Statistics Review, 1975-2016, National Cancer Institute. 2018.
3. Carmeliet P, Jain RK. Angiogenesis in cancer and other diseases. *Nature* 2000; 407: 249-257. DOI:10.1038/35025220.
4. Nishida N, Yano H, Nishida T, Kamura T, Kojiro M. Angiogenesis in cancer. *Vascular Health and Risk Management*. 2006; 2: 213–219. DOI:10.2147/vhrm.2006.2.3.213.
5. Valastyan S, Weinberg RA. Tumor Metastasis: molecular insights and evolving paradigms. *Cell* 2011; 147: 275-292. DOI:10.1016/j.cell.2011.09.024.
6. Hanahan D, Weinberg RA. The hallmarks of cancer. *Cell* 2000; 100: 57–70. DOI: 10.1016/s0092-8674(00)81683-9.
7. Acerbi I, Cassereau L, Dean I, Shi Q, Au A, Park C, Chen YY, Liphardt J, Hwang ES, Weaver V M. Human breast cancer invasion and aggression correlates with ECM stiffening and immune cell infiltration. *Integrative Biology* 2015; 7: 1120–1134. DOI:10.1039/c5ib00040h.
8. Handorf AM, Zhou Y, Halanski MA, Li WJ. Tissue stiffness dictates development, homeostasis, and disease progression. *Organogenesis* 2015; 11: 1–15. DOI:10.1080/15476278.2015.1019687.
9. Lu P, Weaver VM, Werb Z. The extracellular matrix: A dynamic niche in cancer progression. The *Journal of Cell Biology* 2012; 196: 395-406. DOI:10.1083/jcb.201102147.
10. Paszek MJ, Zahir N, Johnson KR, Lakins JN, Rozenberg GI, Gefen A, Reinhart King CA, Margulies SS, Dembo M, Boettiger D, Hammer DA, Weaver VM. Tensional homeostasis and the malignant phenotype. *Cancer Cell* 2005; 8: 241-254. DOI:10.1016/j.ccr.2005.08.010.
11. Wang H, Pan J, Barsky L, Jacob JC, Zheng Y, Gao C, Wang S, Zhu W, Sun H, Lu L, Jia H, Zhao Y, Bruns C, Vago R, Dong Q, Qin L. Characteristics of pre-metastatic niche: the landscape of molecular and cellular pathways. *Mol Biomed*. 2021; 2: 3. doi: 10.1186/s43556-020-00022-z
12. Freeman JW. Structural Biology of the Tumor Microenvironment. *Adv Exp Med Biol*. 2021; 1350: 91-100. doi: 10.1007/978-3-030-83282-7_4.
13. Gupta AA, Kheur S, Palaskar SJ, Narang BR. Deciphering the "Collagen code" in tumor progression. *J Cancer Res Ther*. 2021 ;17: 29-32. doi: 10.4103/jcrt.JCRT_489_17.
14. De Palma M, Biziato D, Petrova TV. Microenvironmental regulation of tumour angiogenesis. *Nat Rev Cancer*. 2017; 17: 457-474. doi: 10.1038/nrc.2017.51
15. Pandya P, Orgaz JL, Sanz-Moreno V. Actomyosin contractility and collective migration: may the force be with you. *Current Opinion in Cell Biology* 2017; 48: 87-96. DOI:10.1016/j.ceb.2017.06.006.
16. Najafi M, Farhood B, Mortezaee K. Extracellular matrix (ECM) stiffness and degradation as cancer drivers. *J Cell Biochem*. 2019; 120: 2782-2790. doi: 10.1002/jcb.27681.
17. Li J, Wu Y, Schimmel N, Al-Ameen MA, Ghosh G. Breast cancer cells mechanosensing in engineered matrices: Correlation with aggressive phenotype. *Journal of the Mechanical Behavior of Biomedical Materials* 2016; 61: 208-220. DOI:10.1016/j.jmbbm.2016.01.021.

18. Dong Y, Xie X, Wang Z, Hu C, Zheng Q, Wang Y, Chen R, Xue T, Chen J, Gao D, Wu W, Ren Z, Cui J. Increasing matrix stiffness upregulates vascular endothelial growth factor expression in hepatocellular carcinoma cells mediated by integrin β1. *Biochemical and Biophysical Research Communications* 2014; 444: 427-432. DOI:10.1016/j.bbrc.2014.01.079.
19. Roy R, Boskey A, Bonassar LJ. Processing of type I collagen gels using nonenzymatic glycation. *Journal of Biomedical Materials Research Part A* 2010; 93: 843–851. DOI:10.1002/jbm.a.32231.
20. Mason BN, Starchenko A, Williams RM, Bonassar LJ, Reinhart-King CA. Tuning three-dimensional collagen matrix stiffness independently of collagen concentration modulates endothelial cell behavior. *Acta Biomaterialia* 2013; 9: 4635–4644. DOI:10.1016/j.actbio.2012.08.007.
21. Doyle AD, Carvajal N, Jin A, Matsumoto K, Yamada KM. Local 3D matrix microenvironment regulates cell migration through spatiotemporal dynamics of contractility-dependent adhesions. *Nat Commun*. 2015; 6: 8720.
22. Ishizaki T, Uehata M, Tamechika I, Keel J, Nonomura K, Maekawa M, Narumiya S. Pharmacological properties of Y-27632, a specific inhibitor of Rho-associated kinases. *Molecular Pharmacology* 2000; 57: 976-983.
23. Kovacs M, Toth J, Hetenyi C, Malnasi-Csizmadia A, Sellers J. Mechanism of Blebbistatin Inhibition of Myosin II. *Journal of Biological Chemistry* 2004; 279; 35557-35563. DOI:10.1074/jbc.M405319200.
24. Shoji K, Oshashi K, Sampei K, Oikawa M, Mizuno K. Cytochalasin D acts as an inhibitor of the actin-cofilin interaction. *Biochemical and Biophysical Research Communications* 2012; 424: 52-57. DOI:10.1016/j.bbrc.2012.06.063.
25. Mierke CT. The matrix environmental and cell mechanical properties regulate cell migration and contribute to the invasive phenotype of cancer cells. *Rep Prog Phys*. 2019; 82: 064602. doi: 10.1088/1361-6633/ab1628
26. Samani A, Bishop J, Luginbuhl C, Plewes DB. Measuring the elastic modulus of ex vivo small tissue samples. *Physics in Medicine and Biology.* 2003, 48, 2183-2189. DOI:10.1088/0031-9155/48/14/310.
27. Nasser M, Wu Y, Danaoui Y, Ghosh G. Engineering microenvironments towards harnessing pro-angiogenic potential of mesenchymal stem cells. *Mater Sci Eng C Mater Biol Appl*. 2019, 102: 75-84.
28. El-Mohri H, Wu Y, Mohanty S, Ghosh G. Impact of matrix stiffness on fibroblast function. *Mater Sci Eng C Mater Biol Appl*. 2017, 74: 146-151.
29. Zhao D, Xue C, Li Q, Liu M, Ma W, Zhou T, Lin Y. Substrate stiffness regulated migration and angiogenesis potential of A549 cells and HUVECs. *J Cell Physiol*. 2018, 233: 3407-3417.
30. Lugano R, Ramachandran M, Dimberg A. Tumor angiogenesis: causes, consequences, challenges and opportunities. *Cellular and Molecular Life Sciences.* 2019; DOI:10.1007/s000018-019-03351-7.
31. Apte RS, Chen DS, Ferrara N. VEGF in signaling and disease: beyond discovery and development. *Cell* 2019; 176: 1248–1264. DOI: 10.1016/j.cell.2019.01.021.
32. Jiang BH, Liu LZ. PI3K/PTEN signaling in angiogenesis and tumorigenesis. *Advances in Cancer Research*. 2009; 102: 19–65. DOI: 10.1016/S0065-230X(09)02002-8.
33. Grose R, Dickson C. Fibroblast growth factor signaling in tumorigenesis. *Cytokine & Growth Factor Reviews* 2005; 16;179-186. DOI:10.1016/j.cytogfr.2005.01.003.

34. Miyake M, Goodison S, Lawton A, Gomes-Giacoia E, Rosser CJ. Angiogenin promotes tumoral growth and angiogenesis by regulating matrix metallopeptidase-2 expression via the ERK1/2 pathway. *Oncogene* 2015; 34: 890–901. DOI:10.1038/onc.2014.2.
35. Dutta D, Ghosh S, Pandit K, Mukhopadhyay P, Chowdhury S. Leptin and cancer: Pathogenesis and modulation. *Indian Journal of Endocrinology and Metabolism.* 2012; 16: S596–S600. DOI:10.4103/2230-8210.105577.
36. Artac M, Altundag K. Leptin and breast cancer: An overview. *Medical Oncology* 2011; 29: 1510-1514. DOI:10.1007/s12032-011-0056-0.
37. Doyle SL, Donohoe CL, Lysaght J, Reynolds JV. Visceral obesity, metabolic syndrome, insulin resistance and cancer. *Proceedings of the Nutrition Society* 2012; 71, 181–189. DOI:10.1017/S002966511100320X.
38. McBryan J, Howlin J, Napoletano S, Martin F. Amphiregulin: role in mammary gland development and breast cancer. *J Mammary Gland Biol Neoplasia*. 2008; 13:159-69. doi: 10.1007/s10911-008-9075-7
39. Riehl BD, Kim E, Bouzid T, Lim JY. The Role of Microenvironmental Cues and Mechanical Loading Milieus in Breast Cancer Cell Progression and Metastasis. *Front Bioeng Biotechnol*. 2021; 8: 608526. doi: 10.3389/fbioe.2020.608526.
40. Fletcher DA, Mullins RD. Cell mechanics and the cytoskeleton. *Nature* 2010; 463: 485–492. DOI:10.1038/nature08908.
41. Wang A, Ma X, Conti MA, Adelstein RS. Distinct and redundant roles of the non-muscle myosin II isoforms and functional domains. *Biochemical Society Transactions* 2011; 39: 1131–1135. DOI:10.1042/BST0391131.

Figure Captions

Figure 1. (A) Degradation of non-glycated and glycated collagen gels monitored over 10 days. Error bar S.E.M (N=3). (B)Scanning electron microscope images of collagen network. (C) Percentage of dextran released from collagen gels (0 mM and 250 mM) over 7 days. Inset shows the release of dextran at early time points. Error bar S.E.M (N=3).

Figure 2. MDA-MB-231 cancer cells were encapsulated in soft (0 mM) and stiff (250 mM) collagen matrices, and the impact of matrix mechanics on proliferation and morphology was investigated. (A) Proliferation of MDA-MB-231 cells in glycated and non-glycated gels was assessed after 2, 4, and 6 days and compared to the day of fabrication. Error bar S.E.M (N=3) (*p-value<0.05 in comparison to day 0). (B) The confocal images of the cells displaying the arrangement of actin fibers (green). Hoechst 33342 (blue) stained the nuclei of the cells. The scale bar corresponds to 50 μm.

Figure 3. Effect of matrix stiffness on angiogenic activity of MDA-MB-231 cells. The mean pixel density of (A) pro-angiogenic factors and (B) anti-angiogenic factors released by MDA-MB-231 cells encapsulated in non-glycated (0 mM ribose) and glycated (250 mM ribose) collagen gels assayed via Angiogenesis Proteome Profiler. (C-D). The expression of angiogenesis-related factors released by MDA-MB-231 encapsulated within glycated gels was normalized with respect to those released from non-glycated gels. The normalized expression of (C) pro-angiogenic factors and (D) anti-angiogenic factors. The closely dashed and widely dashed lines corresponds to the relative expression of 0.5 and 1.5, respectively. (E) The proliferation of HUVECs in the presence of conditioned media collected at Day 4 was normalized with respect to that in presence of HUVECs media (control). Error bar S.E.M (N=3).

Figure 4. Effect of mechanotransduction inhibitors on angiogenic signaling of MDA-MB-231 encapsulated in stiff (250 mM) collagen gels. (A) The normalized expression of pro-angiogenic factors in the presence of inhibitors relative to the signals released by cells in the absence of inhibitors. (B) The cell viability of MDA-MB-231 cells incubated with and without inhibitors was not affected.

Figure 1

A

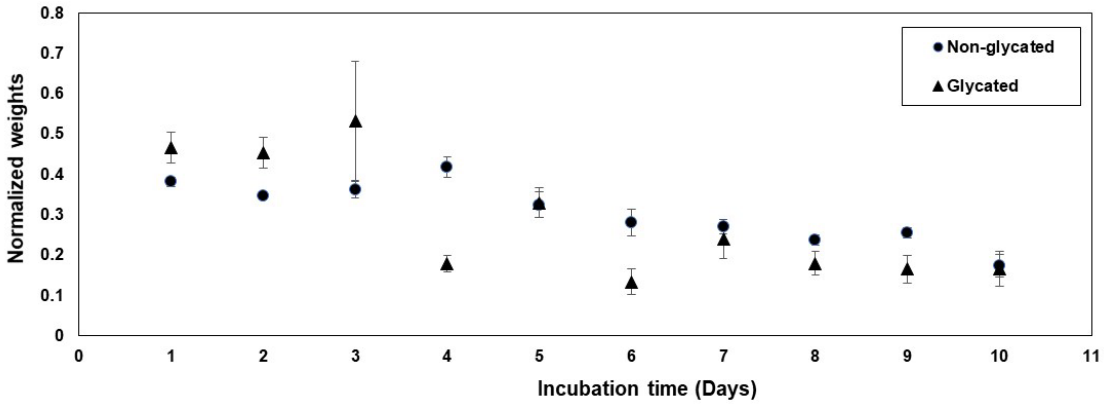

B

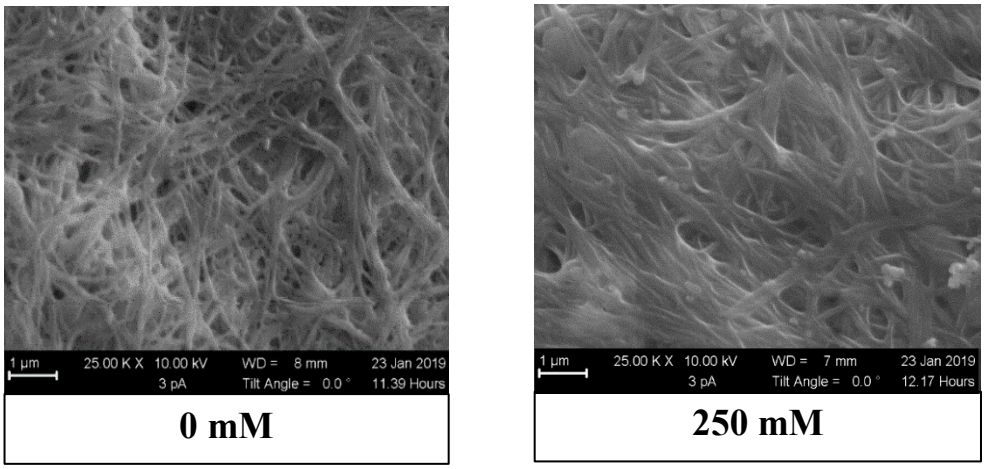

C

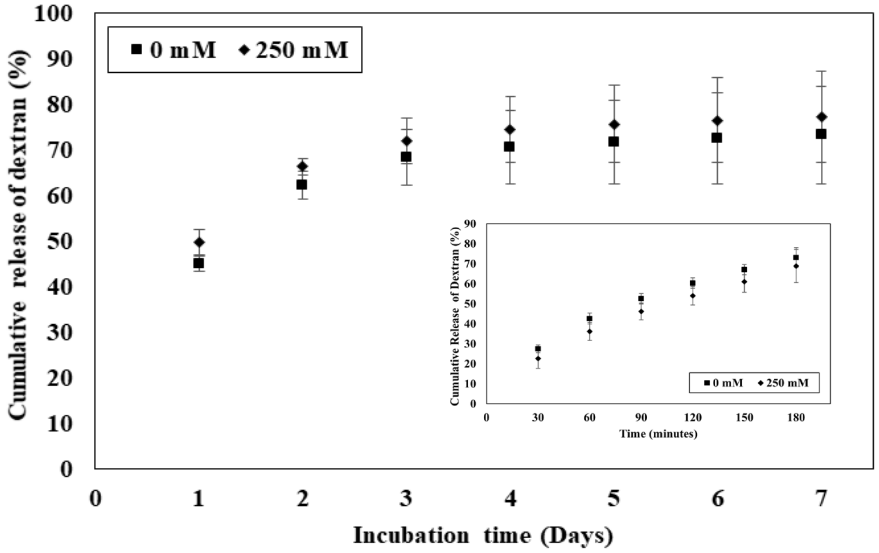

Figure 2

A

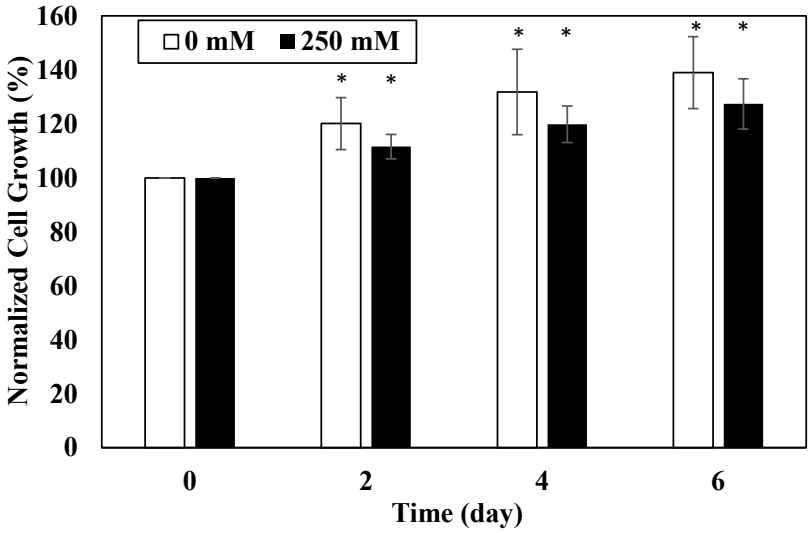

B

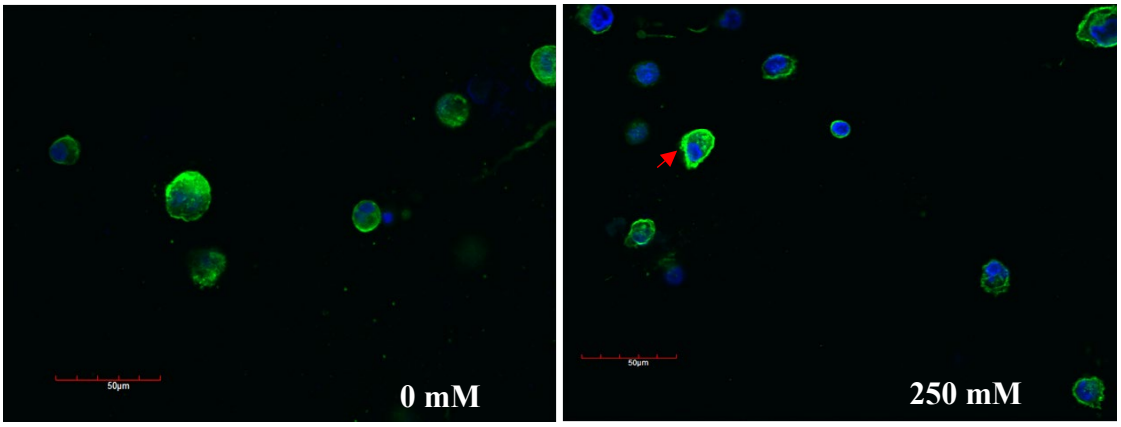

Figure 3

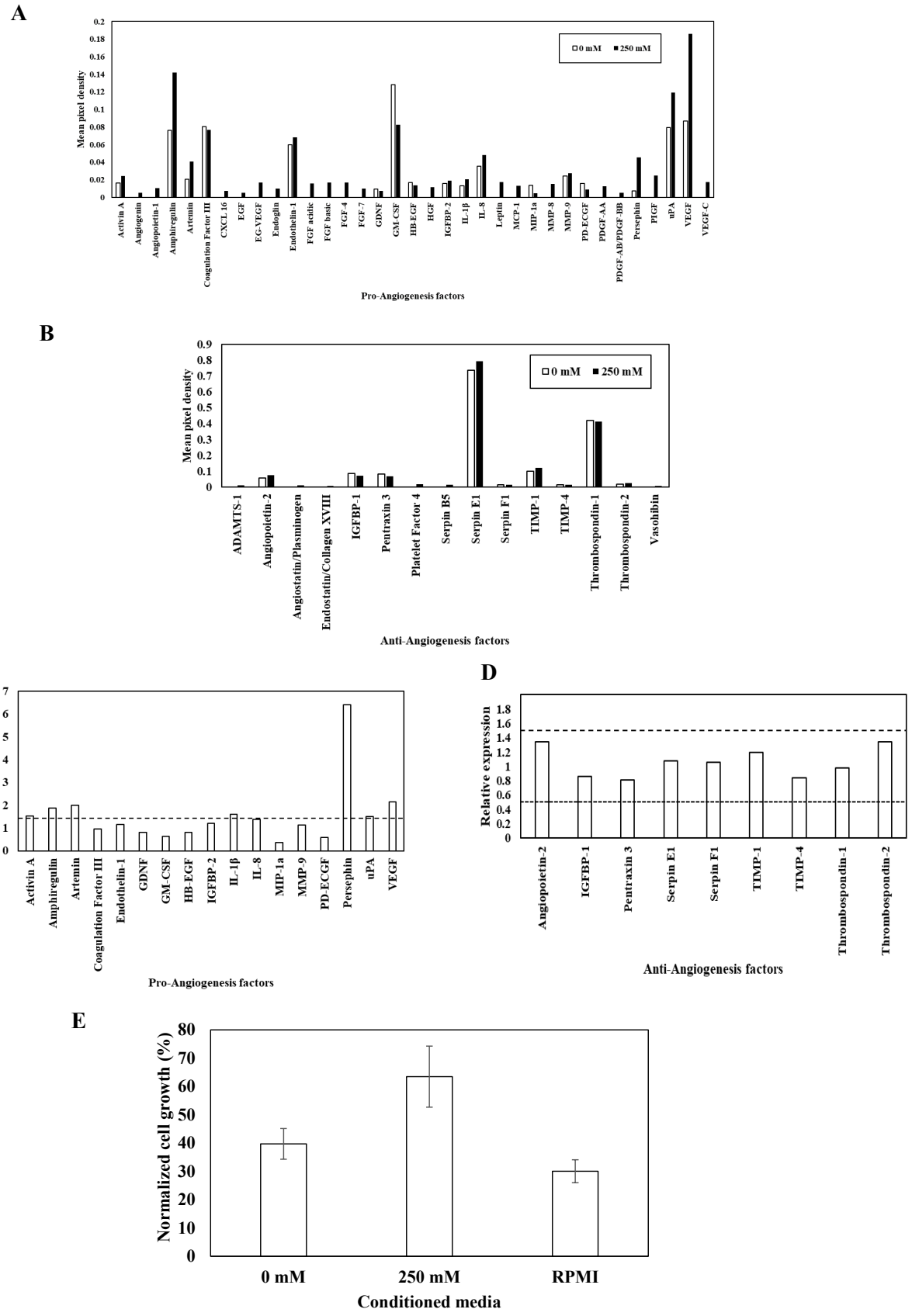

Figure 4

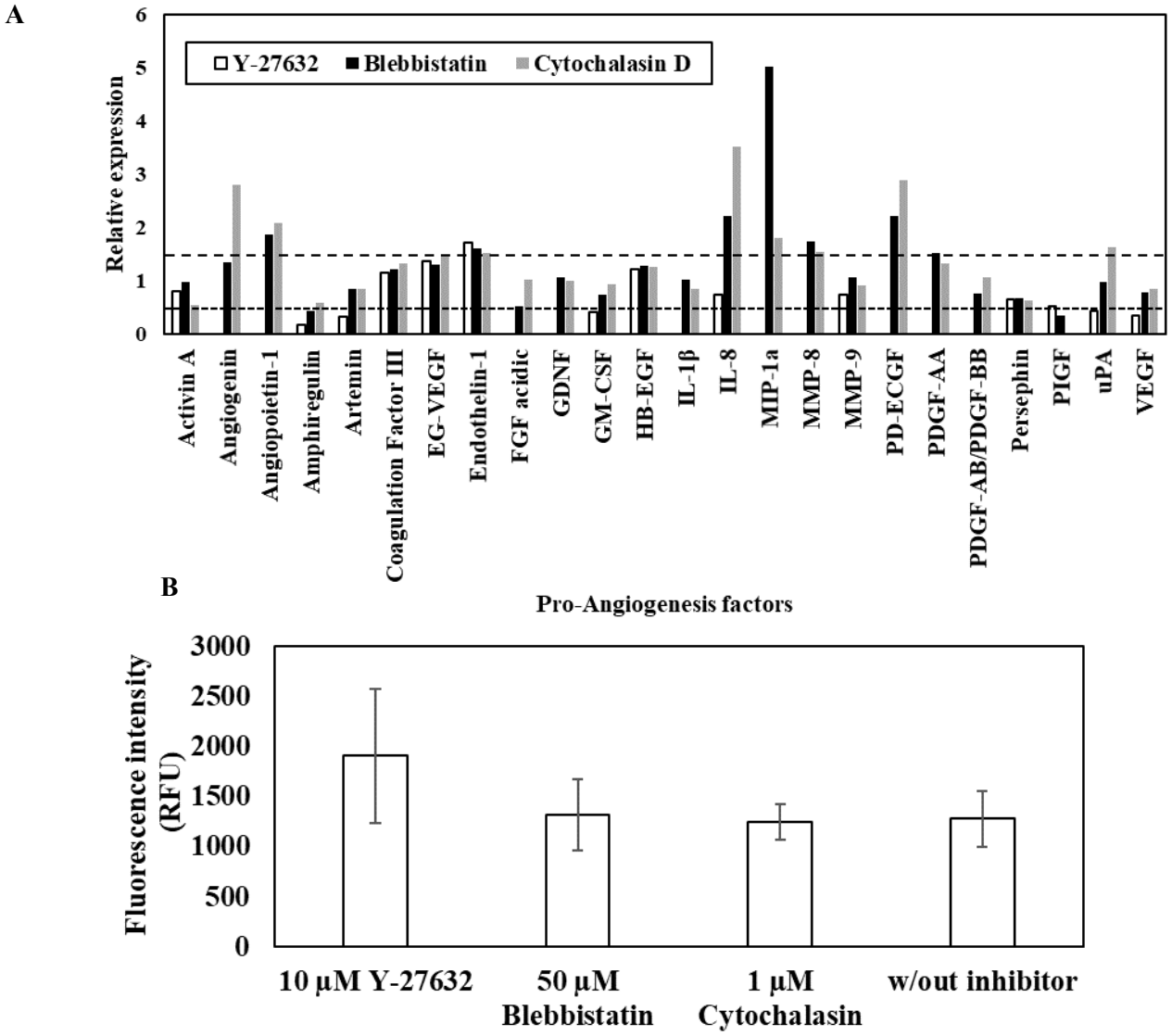

Table 1. Comparison of correlation coefficients for different kinetic models and diffusion exponent as a function of collagen glycation.

Ribose Concentration	Zero-order	First Order	Higuchi Model	Korsemeyer-Peppas model	Diffusion exponent
0 mM	0.8147	0.5774	0.9933	0.9843	0.567838 ± 0.031
250 mM	0.8399	0.6119	0.9984	0.9919	0.627931 ± 0.009